

Knockout reaction induced by ${}^6\text{He}$ at 61.2 MeV/u^{*}

LÜ Lin-Hui(吕林辉)¹ YE Yan-Lin(叶沿林)^{1;1)} JIANG Dong-Xing(江栋兴)¹ HUA Hui(华辉)¹
 ZHENG Tao(郑涛)¹ LI Zhi-Huan(李智焕)¹ GE Yu-Cheng(葛愉成)¹ LI Xiang-Qing(李湘庆)¹
 LOU Jian-Ling(楼建玲)¹ CAO Zhong-Xin(曹中鑫)¹ SONG Yu-Shou(宋玉收)¹ XIAO Jun(肖军)¹
 LI Qi-Te(李奇特)¹ QIAO Rui(乔锐)¹ YOU Hai-Bo(游海波)¹ CHEN Rui-Jiu(陈瑞久)¹
 XU Hu-Shan(徐珊珊)² WANG Jian-Song(王建松)² GUO Zhong-Yan(郭忠言)²
 ZHANG Xue-Ying(张雪荧)² LI Chen(李琛)² HU Zheng-Guo(胡正国)²
 CHEN Ruo-FU(陈若富)² WANG Meng(王猛)² XU Zhi-Guo(徐治国)² YUE Ke(岳珂)²
 TANG Bin(唐彬)² ZANG Yong-Dong(臧永东)² ZHANG Xue-Heng(章学恒)²
 YAO Xiang-Wu(姚向武)² CHEN Jin-Da(陈金达)² BAI Zhen(白真)²

¹ School of Physics and State Key Laboratory of Nuclear Physics and Technology, Peking University, Beijing 100871, China

² Institute of Modern Physics, Chinese Academy of Sciences, Lanzhou 730000, China

Abstract: A knockout reaction induced by ${}^6\text{He}$ at 61.2 MeV/u was carried out at the HIRFL-RIBLL radioactive beam line. The α core fragments at forward angles were detected in coincidence with the recoiled protons at large angles. From this coincident measurement the valence nucleon knockout mechanism and the core knockout mechanism can be separated according to the polar angle correlation between the core fragments and the recoiled protons. It is demonstrated that, when reconstructing the resonant state of a weakly bound nucleus, the contamination resulting from the core knockout mechanism should be eliminated in order to obtain the correct structure information.

Key words: halo nucleus, knockout reaction, reaction mechanism, invariant mass spectra

PACS: 25.60.-t, 24.50.+g, 25.70.Mn **DOI:** 10.1088/1674-1137/35/10/001

1 Introduction

The knockout reaction plays an important role in probing the single-particle and cluster structure of stable nuclei [1]. Since the advent of fast radioactive nucleus beams, the knockout reaction with inverse kinematics has been developed into a powerful tool for spectroscopic investigation of the exotic properties of unstable nuclei [2]. It is well known that, due to the weak binding property of unstable nuclei, most structure information may have to be extracted from reaction experiments. Therefore a clear understanding of the reaction mechanism is important not only for its own sake but also for structure studies[3]. Very recently an unexpected resonance peak around 0.6 MeV above the ground state of ${}^7\text{He}$ was reported

from a knockout reaction experiment using a carbon target [4] but could not be confirmed in a similar experiment using a hydrogen target [5]. Furthermore the strong reduction of the spectroscopic factor (SF) for weakly bound nuclei observed in knockout reactions is not consistent with that observed in transfer reactions [6, 7], which might be attributed to some reaction mechanism problems.

${}^6\text{He}$ is the lightest neutron halo nucleus with the so-called borromean configuration, to which continuous attention has been paid both experimentally and theoretically [8–16]. Its structure is well understood and described as an α core plus two valence neutrons, both in the $(0p_{3/2})$ state. Due to its simple and well studied structure, ${}^6\text{He}$ is a good test case for the study of the reaction mechanism. Early in the 1990s the

Received 23 May 2011

^{*} Supported by National Basic Research Program (973 Program) of China (2007CB815002), and National Natural Science Foundation of China (11035001, 10775003, 10827505, J0730316)

1) E-mail: yeyl@pku.edu.cn

©2011 Chinese Physical Society and the Institute of High Energy Physics of the Chinese Academy of Sciences and the Institute of Modern Physics of the Chinese Academy of Sciences and IOP Publishing Ltd

reaction mechanism of a fast-moving borromean-type projectile was schematically described [17, 18], including the knockout of a valence nucleon followed by resonance decay and the knockout of the core fragment (cluster) followed by emission of valence nucleons. In subsequent studies the latter mechanism was often neglected, based on the strong absorption assumption for experiments employing composite targets (such as beryllium or carbon targets) [2]. But, as demonstrated in a quasi-free scattering experiment with ${}^{6,8}\text{He}$ beams impinging on a non-absorptive hydrogen target [14], the coincident measurement of the recoiled proton allows us to clearly identify the core fragment knockout process, which in turn could be used to study the cluster structure of the projectile at ground state. That experiment was carried out at very high energy (717 MeV/u for ${}^6\text{He}$) and did not employ neutron detection. It would be interesting to investigate the validity of this separation of the core knockout reaction mechanism at energies below 100 MeV/u where many knockout experiments for unstable nuclei have been performed and much spectroscopic information has been acquired.

We report here an experiment of a knockout reaction using a 61.2 MeV/nucleon ${}^6\text{He}$ beam impinging on a CH_2 target. The goal is to possibly distinguish the valence neutron knockout and the core fragment knockout mechanisms, by the coincident measurement of the emitted ${}^4\text{He}$ particles with the recoiled protons. Also, possible contamination from the core knockout mechanism to the reconstructed resonance spectrum is checked.

2 Experimental details

The experiment was carried out at the Heavy Ion Research Facility in Lanzhou (HIRFL). An 85 MeV/nucleon ${}^{13}\text{C}$ primary beam was supplied by the SSC cyclotron. Secondary ${}^6\text{He}$ ions at 61.2 MeV/nucleon were produced from a 4.5 mm thick ${}^9\text{Be}$ primary target and transported by the Radioactive Ion Beam Line in Lanzhou (RIBLL) [19] to a vacuum chamber where the physics target CH_2 and detector system were installed. The secondary beam particles were identified by the time of flight (TOF) and energy loss detected by the beam monitors. As shown in Fig. 1 the secondary beam is composed of about 81.3% ${}^6\text{He}$ and some contaminants of ${}^9\text{Li}$ and ${}^3\text{H}$ at a 20% level. In addition a parallel-plane avalanche counter (PPAC3) was installed at the F3 focal plane of the beam line to monitor the beam profile. The secondary beam intensity was about 1×10^4

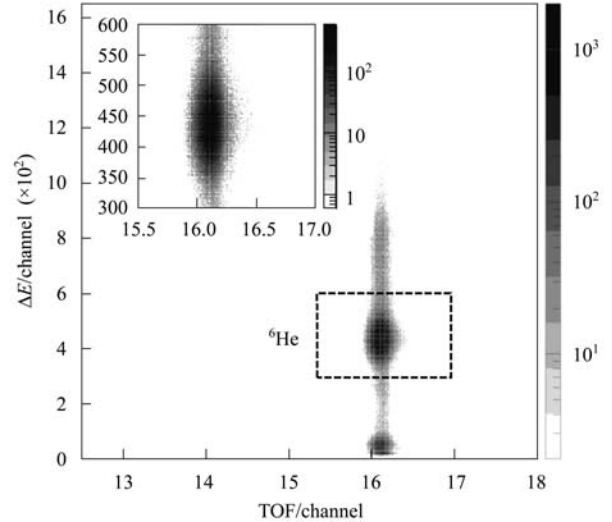


Fig. 1. Particle identification according to the TOF measured by scintillation counters along the beam line and energy loss measured by a thin silicon detector upstream from the target.

particles per second.

As shown in Fig. 2 two parallel-plate avalanche counters PPAC1 and PPAC2 and a double-sided silicon strip detector (0.5 mm thickness) were set upstream of the target in order to measure the incident angle of the projectiles. A CH_2 target with a diameter of 30 mm and a thickness of 85.19 mg/cm² was used as the physics target. Downstream of the target, charged fragments at forward angles were detected by the telescopes D0 and D2, and the recoiled protons were detected by D11 and D12 at larger angles according to the kinematics calculation. Each telescope was composed of a position-sensitive detector (double-sided silicon strip layers for D0 and D12, and position-sensitive detector for D2), an energy loss detector (thin CsI(Tl) crystal for D11 and D0, and a large-area silicon layer for D12, D2) and a stop detector (thick CsI(Tl) crystal for all telescopes). The size, shape and thickness of the energy loss detectors and the stop detectors were optimized according to Monte Carlo simulation. D11 and D12 played also a key role in triggering the data-collecting system and were crucial for selecting the different reaction processes. The D0 telescope covered $\pm 6^\circ$ around the beam line. The D2 telescope covered 7° – 17° to detect fragments at relatively larger angles. Good particle identification performance was obtained for all telescopes as shown in Fig. 3.

Neutrons emitted at forward angles were detected by an array of four layers of plastic scintillator (not shown in the figure). The first layer was positioned at a distance of 350 cm downstream the target, and

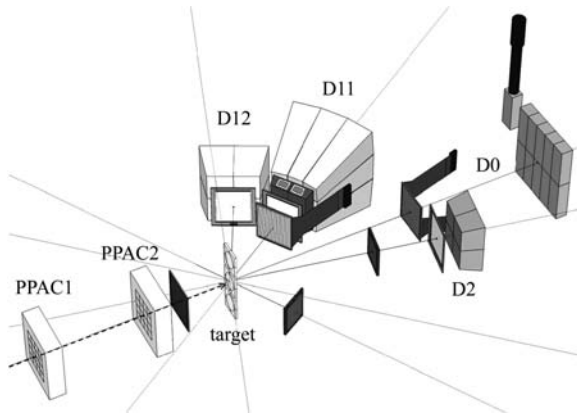


Fig. 2. Experimental setup in the vacuum chamber. D11 and D12 are telescopes used to detect the recoil protons, and D0 and D2 to detect the charged fragments.

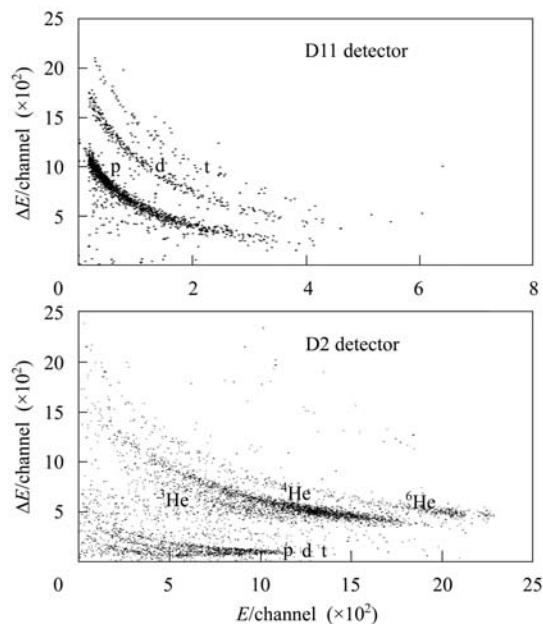


Fig. 3. Particle identification performance for telescopes D11 and D2.

the other layers were separated from each other by 50 cm. In total 24 scintillation bars were used. The bar in the first and second layers had dimensions of 100 cm \times 5 cm \times 6 cm, while that in the third and fourth layers had a size of 144 cm \times 8 cm \times 8 cm. Both ends of each bar were coupled to photomultiplier tubes (PMT). The active area of the first and second layer amounted to 1 m \times 1 m, covering an angular range of about 14°. In each layer the bars were stacked horizontally and separated from each other by a space equal to the bar width. This configuration was adopted in order to test the cross-talk rejection performance which is important for two-neutron coincident detection [20, 21]. One veto wall composed of a thin plastic scintillator was installed in front of

the neutron array, in order to reject the charged particles. The neutron time of flight was obtained from the time difference between the beam timing signal and the mean time of the two PMTs collected at both ends of a fired neutron bar. The horizontal position of a striking neutron was determined from the time difference between the two PMT signals and the vertical position was decided just by the bar position. For a 60 MeV neutron the energy resolution is 4.3% (FWHM), and the neutron detection efficiency for the whole array is about 10%, estimated from the test measurement and the Monte Carlo simulation.

3 Results and discussion

The coincident measurement of the forward He fragments and the recoiled protons were analyzed event by event. Firstly we select ${}^4\text{He}$ fragments from the D0 or D2 telescope, and look for the coincident protons in D11 and D12. The precise positions of these particles are obtained from the corresponding position-sensitive detector in the telescope. From these positions the scattering polar angle relative to the incident angle can be deduced. Shown in Fig. 4 is the distribution of the proton polar angle versus the ${}^4\text{He}$ polar angle. It should be noted that the empty slice at around 45° of the proton angle is a result of the dead area between D11 and D12. But for the ${}^4\text{He}$ polar angle, the detector dead area between D0 and D2 is much smaller (only between 6° and 7°) and the empty slice at around 7.5° results from the reaction mechanisms.

For the mechanism of a valence neutron knockout, the ${}^4\text{He}$ core fragment is almost untouched and should fly out along the beam line with an angular spread determined by its Fermi motion in the mother nucleus ${}^6\text{He}$. This mechanism is represented by the events concentrated at the left side of the figure (close to zero degrees of the ${}^4\text{He}$ polar angle). On the other hand, if the quasi-free core knockout occurs the ${}^4\text{He}$ fragment will fly to a larger angle and should follow approximately the kinematics of free ${}^4\text{He}+p$ scattering as shown in the figure by the black curve. This mechanism is indicated by events concentrated in the middle part in Fig. 4. This kind of separation of the reaction mechanism was already realized at very high energy (717 MeV/u) [14], with proton detectors at angles close to 90° to avoid the difficulty of very high energy detection. We demonstrate here that this separation of the reaction mechanism can also be realized at much lower energies where the beam availability is much better assured and the proton detection may be

realized to large angular range by the use of normal particle telescopes.

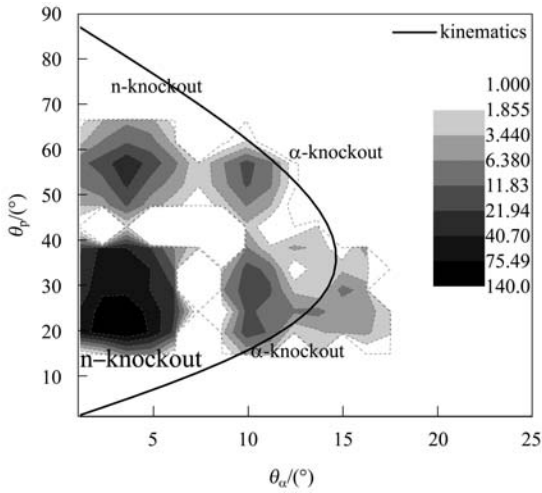


Fig. 4. Polar angle correlation between the core fragment and the recoiled proton, from which the n-knockout and α -knockout reaction mechanisms are separated.

For more than a decade the knockout reaction has been used extensively to extract SF for resonant states or bound states. In the former case the resonance after the removal of the valence nucleons will undergo a decay into two or more particles which can be detected and used to reconstruct the relative energy (invariant mass) spectrum. In principle only the valence nucleon knockout mechanism should be included, without contamination from the core knockout process. In our case this means selecting events with small ^4He polar angle as shown in Fig. 4. Shown in Fig. 5 is the invariant mass of ^5He reconstructed from the small-angle ^4He and the coincident neutron. The peak at about 0.9 MeV and the shape of the resonance are in agreement with the previous measurements [22]. In contrast if we select the core knockout mechanism corresponding to the part with larger ^4He polar angles, a quite different invariant mass spectrum for ^5He is obtained, as shown in Fig. 6. In addition to a peak at about 1 MeV, another broad structure peaking at about 2.8 MeV appears with high probability. Of course the core knockout mechanism should be excluded from the study of the ^5He structure because it is strongly modified by the knockout process. In previous studies the measurements were inclusive with respect to the knockout mechanism and therefore some unexplained structure might appear. Due to the relatively low beam intensity, and therefore poor statistics, we were not able to distinguish the contribution from the carbon or the hydrogen target. But the comparison of the reconstructed spectra

from the same measurement is meaningful to illustrate the importance of eliminating the contamination caused by the core knockout reaction process.

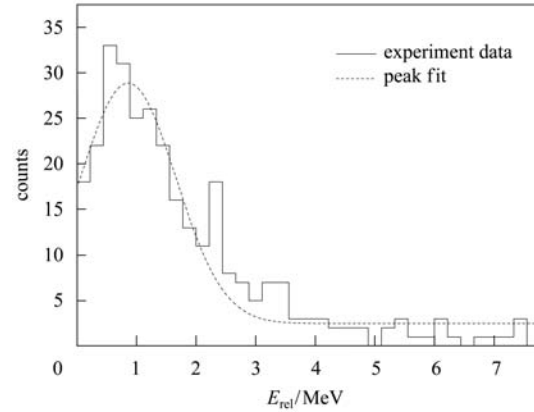


Fig. 5. Invariant mass spectrum reconstructed from ^4He fragments with very small polar angle, corresponding to the nucleon knockout mechanism, and the coincident single neutron measured by the neutron array. The fit gives a resonance centered at $E_r = 0.86$ MeV and with a width $\Gamma_r = 0.81$ MeV.

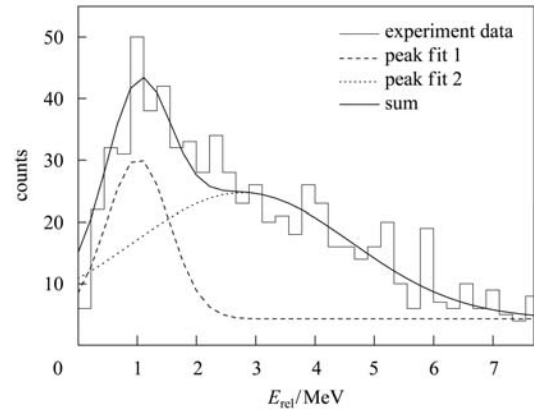


Fig. 6. The “fake” invariant mass spectrum reconstructed from the ^4He fragments corresponding to the core knockout mechanism and the coincident neutrons detected by the neutron wall. The fit gives two resonances with $E_r = 1.01$ MeV, $\Gamma_r = 1.05$ MeV and $E_r = 2.78$ MeV, $\Gamma_r = 3.68$ MeV, respectively.

4 Summary

A knockout reaction experiment was carried out for a ^6He beam at 61.2 MeV/u impinging on a CH_2 target. the α core fragments at forward angles were detected in coincidence with the recoiled protons at larger angles. From this exclusive measurement the valence nucleon knockout mechanism and the

core knockout mechanism can be separated based on the correlation between the polar angles of the core fragments and the recoiled protons, respectively. It is demonstrated that the core knockout mechanism might result in some strong contamination of the real invariant mass spectrum and even create a “fake” resonance peak in the larger mass region. Therefore it is very important to test and clarify the knockout reac-

tion mechanism before using it to extract the structure information of exotic nuclei. This should also be true for the study of bound states of exotic nuclei, where the parallel momentum distribution of the core fragment is often measured based on the assumption of a perfect spectator. This momentum distribution might also be biased if the core knockout mechanism is included in the measurement.

References

- 1 Roos P G et al. *Phys. Rev. C*, 1977, **15**: 69
- 2 Hansen P G, Tostevin J A. *Annu. Rev. Nucl. Part. Sci.*, 2003, **53**: 219
- 3 Suzuki Y, Lovas R G, Yabana K, Varga K. *Structure and reaction of light exotic nuclei*. London: Taylor and Francis, 2003, 3
- 4 Markenroth K et al. *Nucl. Phys. A*, 2001, **679**: 462
- 5 Aksyutina Yu et al. *Phys. Lett. B*, 2009, **679**: 191
- 6 Dickhoff W H. *J. Phys. G*, 2010, **37**: 064007
- 7 Lee J, Tsang M B, Bazin D et al. *Phys. Rev. Lett.*, 2010, **104**: 112701
- 8 Tanihata I et al. *Phys. Rev. Lett.*, 1985, **55**: 2676–2679
- 9 Tanihata I, Hirata D, Kobayashi T et al. *Phys. Lett. B*, 1992, **289**: 261–266
- 10 Zhukov M V, Danilin B V, Fedorov D V et al. *Phys. Report*, 1993, **231**: 151–199
- 11 Wurzer J, Hofman H M. *Phys. Rev. C*, 1997, **55**: 688–698
- 12 Jonson B. *Nucl. Phys. A*, 1998, **631**: 376c–386c
- 13 Oganessian Y T, Zagrebaev V I. *Phys. Rev. Lett.*, 1999, **82**: 4996–4999
- 14 Chulkov L V, Aksouh F, Bleile A et al. *Nucl. Phys. A*, 2005, **759**: 43–63
- 15 YE Y L, PANG D Y, JIANG D X et al. *Phys. Rev. C*, 2005, **71**: 014604
- 16 Kikuchi Y, Kato K et al. *Phys. Rev. C*, 2010, **81**: 044308
- 17 Korshennikov A A, Kobayashi T. *Nucl. Phys. A*, 1994, **567**: 97
- 18 Korshennikov A A et al. *Europhys. Lett.*, 1995, **29**: 359
- 19 SUN Z, ZHAN W L, GUO Z Y et al. *Nucl. Instrum. Methods Phys. Res. A*, 2003, **503**: 496
- 20 Marques F M, Labiche M, Orr N A et al. *Nucl. Instrum. Methods Phys. Res. A*, 2000, **450**: 109
- 21 WANG J, Galonsky A, Kruse J J et al. *Nucl. Instrum. Methods Phys. Res. A*, 1997, **397**: 380
- 22 Aleksandrov D, Aumann T, Axelsson L et al. *Nucl. Phys. A*, 1998, **633**: 234